Molecular Structure and Torsional Potential of *trans*-Azobenzene. A Gas Electron Diffraction Study

Takemasa Tsuji, Hiroyuki Takashima, Hiroshi Takeuchi, Toru Egawa, and Shigehiro Konaka*

Division of Chemistry, Graduate School of Science, Hokkaido University, Sapporo 060-0810, Japan

Received: December 7, 2000; In Final Form: August 6, 2001

The molecular structure of *trans*-azobenzene (Ph−N═N−Ph) has been determined by gas electron diffraction. Diffraction patterns were taken at 407 K and data analysis was made using the structural constraints obtained from MP2/6-31+G* calculations. Vibrational mean amplitudes and shrinkage corrections were calculated from the harmonic force constants given by a normal coordinate analysis. Vibrational mean amplitudes were refined as groups. The torsion of each phenyl ring was treated as a large amplitude vibration. The potential function for torsion was assumed to be $V(\phi_1,\phi_2) = \Sigma_{i=1,2}\{V_2(1 - \cos 2\phi_i)/2 + V_4(1 - \cos 4\phi_i)/2\}$, where ϕ_i denotes the torsional angle around each N−C bond. Quantum mechanical calculations were performed by taking account of two torsional motions to derive a probability distribution function, $P(\phi_1,\phi_2)$. Because $P(\phi_1,\phi_2) = N \exp(-V(\phi_1,\phi_2)/kT)$ was found to be a good approximation at 407 K where N is a constant, it was adopted in the data analysis. The determined potential constants (V_2 and V_4/kcal mol^{-1}) and principal structure parameters (r_g/Å, $\angle_\alpha$/deg) with the estimated limits of error (3σ) are as follows: $V_2 = 1.7(6)$; $V_4 = 0.6(13)$; r(N═N) = 1.260(8); r(N−C) = 1.427(8); $\langle r(\text{C−C})\rangle = 1.399(1)$; $\langle r(\text{C−H})\rangle = 1.102(7)$; ∠NNC = 113.6(8); $(\angle\text{NCC}_{cis} - \angle\text{NCC}_{trans})/2 = 5.0(9)$, where $\langle\ \rangle$ means an average value and C_{cis} and C_{trans} denote the carbon atoms cis and trans to the N═N bond, respectively. Thus, the stable form was found to be planar with C_{2h} symmetry. The observed structure was compared with those of *trans*-azoxybenzene (Ph−N(−O)═N−Ph) and *trans*-stilbene (Ph−CH═CH−Ph). The stability of the liquid crystals with these types of molecular cores was discussed on the basis of the gas-phase structures of the model compounds of cores. Nearly the same results were obtained in the data analysis using the constraints from RHF/6-31G** ab initio calculations.

Introduction

Recently, we have determined the molecular structures of *p*-azoxyanisole (PAA) and *N*-(4-methoxybenzylidene)-4'-*n*-butylaniline (MBBA) by gas electron diffraction (GED).[1,2] These compounds are mesogens, that is, they can form liquid crystals. The structure of the rigid central part (core) of each liquid-crystal molecule is an important factor to determine the nematic to liquid-phase transition temperature, T_{N-I}.[3] In ref 2, the high T_{N-I} of PAA as compared with MBBA was discussed qualitatively on the basis of the conformations of the cores. More structural data of mesogens are required to investigate the relation between the gas-phase structures and T_{N-I}. However, the complexity and flexibility of liquid-crystal molecules make their structure determination quite a time-consuming task and prevent us from going to a comprehensive study.

The gas-phase structure of the core of the PAA molecule[1] was found to agree with that of *trans*-azoxybenzene (*t*-AXB),[4] which is a model compound of the molecular core of PAA. Moreover, the gas-phase structure of the core of MBBA[2] is quite similar to that of *N*-benzylideneaniline,[5] a model compound of the core of MBBA. It is reasonable to expect that the structural similarity between the mesogen and its model compound holds also for other cores, and thus we can discuss the relationship between the structures of the model compounds of cores and T_{N-I}.

* To whom correspondence should be addressed. Fax: +81-11-706-2699. E-mail: konaka@sci.hokudai.ac.jp.

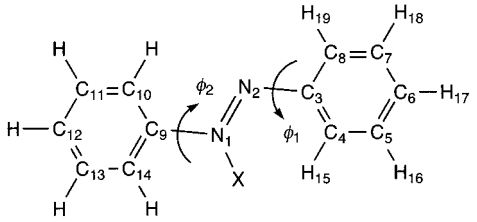

Figure 1. Molecular models with atom numbering of *trans*-azobenzene (X = none) and *trans*-azoxybenzene (X = O). ϕ_1 and ϕ_2 denote dihedral angles $N_1N_2C_3C_4$ and $N_2N_1C_9C_{10}$, respectively. They are defined to be 0° for the planar conformer given here.

The molecule of *trans*-azobenzene (*t*-AB, Figure 1) is a model of the molecular core of the mesogens of *t*-AB type (R−C_6H_4−N═N−C_6H_4−R'), where R and R' are flexible groups. As shown in Figure 1, *t*-AB is very similar to *t*-AXB and is an isoelectronic molecule of *trans*-stilbene (*t*-SB), which is a model compound of another core. The T_{N-I} of the mesogens of *t*-AB type is lower than those of *t*-AXB and *t*-SB types by about 20 and 30 °C on average, respectively, for common terminal substituents.[6,7] For example, when the terminal groups are ethoxy groups, T_{N-I} is 142, 168, and 189 °C for *t*-AB, *t*-AXB, and *t*-SB types, respectively.[8] Therefore, it is interesting to compare the structure of *t*-AB with *t*-AXB and *t*-SB to find out which part of the geometry affects the difference in T_{N-I}.

About two decades ago, the molecular structure of *t*-AB was investigated by gas electron diffraction.[9] According to this investigation, the dihedral angle between each phenyl ring and

10.1021/jp004418v CCC: $20.00
Published on Web 09/19/2001

the CNNC plane is about 30°, but the authors could not conclude whether the two phenyl rings rotate in the same direction ($\phi_1 = -\phi_2 \neq 0°$) to result in the molecular symmetry of C_i or in the opposite direction ($\phi_1 = \phi_2 \neq 0°$) to give C_2 symmetry.[9] This is probably because it was impossible to perform the precise data analysis using the structural constraints from ab initio calculations and treating a large amplitude vibration for such a molecule with many atoms. Recently, the progress in the computational resources has made it more practical than before to carry out ab initio calculations and calculations based on density functional theory (DFT) for relatively large molecules. Thus, we decided to perform a GED experiment on *t*-AB to determine a more reliable structure with the aid of theoretical calculations.

Several X-ray diffraction data are available for the crystal structure of *t*-AB.[10−13] There are two crystallographically independent sites in the crystal. The symmetry group of the *t*-AB molecule in the crystal is C_i, and the phenyl rings rotate from the CNNC plane by 5−20°. A recent study revealed that the internal rotations of the phenyl rings cause dynamic disorder at one site at room temperature.[13]

The *t*-AB molecule is considered to have C_i symmetry or take a planar conformation with C_{2h} symmetry in solutions.[14−17] The vibrational spectra of *t*-AB and its isotopically substituted derivatives were measured in solutions.[14,15] From the depolarization ratios of Raman lines measured in a solution, Kellerer et al.[14] concluded that the *t*-AB molecule has C_i symmetry. Armstrong et al.[16] performed structure optimizations and normal coordinate analyses by ab initio RHF and MP2 calculations using various basis sets. Their optimizations assuming C_i symmetry resulted in C_{2h} symmetry ($\phi_1 = \phi_2 = 0°$). The vibrational wavenumbers given by the MP2 calculations assuming C_{2h} symmetry were in good agreement with the measured ones in solutions. Recently, DFT calculations were successfully used for reproducing vibrational spectroscopic data.[17−20] Biswas and Umapathy[17] reported the results of normal coordinate analyses of *t*-AB by various DFT calculations using the 3-21G, 6-31G, and 6-31G* basis sets. The optimizations by DFT calculations showed that *t*-AB has C_i symmetry and that the distortion from planarity is slight.[17] The BP86/6-31G* calculations[21,22] give more accurate vibrational wavenumbers than other DFT calculations.[17] Very recently, Kurita et al.[23] performed the structural optimizations and vibrational calculations of *t*−AB and *cis*−azobenzene by using a variety of methods (HF, MP2, and DFT) and basis sets. Among the structural optimizations of *t*-AB, only the MP2/6-31+G* calculation resulted in the nonplanar structure with $\phi_1 = \phi_2 = 18.5°$.[23]

The principal purpose of the present study is to determine the accurate molecular structure of *t*-AB by GED. In the data analysis, constraints from ab initio MO calculations have been used to resolve closely spaced interatomic distances, and the torsion of each phenyl ring has been treated as a large amplitude vibration to obtain a potential function. Determined structure parameters are compared with those of *t*-AXB and *t*-SB and the differences in the T_{N-I} of liquid crystals are discussed on the basis of the gas-phase structures of the model compounds of cores.

Experimental Section

A commercial sample with a purity of better than 98% (Merck−Schuchardt) was used without further purification. Electron diffraction patterns were recorded on 8 × 8 in. Kodak projector slide plates by using an apparatus with an r^3-sector[24] and a high-temperature nozzle.[1] The temperature of the nozzle tip was about 407 K during exposures, and the camera distance was 244.3 mm. The accelerating voltage of incident electrons was about 38 kV. The diffraction patterns of carbon disulfide were recorded in the same sequence of exposures as the sample. The scale factor was calibrated to the known bond length of carbon disulfide (r_a(C−S) = 1.5570 Å).[25] Other experimental conditions are as follows: electron wavelength, 0.06326 Å; uncertainty in the scale factor (3σ), 0.04%; exposure time, 60−70 s; beam current, 1.6 μA; background pressure during exposure, 4×10^{-6} Torr.

Data reduction was carried out as described in ref 2. Total intensities from three plates were averaged and used in the analysis. Average total intensities and backgrounds are available as Supporting Information (Table S1). Elastic atomic scattering factors were calculated as described in ref 26, and inelastic ones were taken from ref 27.

Theoretical Calculations

Calculations were performed with the programs GAUSSIAN 94[28a] and 98.[28b] Geometrical parameters were fully optimized by RHF/6-31G** and MP2/6-31+G* calculations. In the RHF/6-31G** calculations, the optimization starting from a nonplanar structure resulted in an essentially planar one with C_{2h} symmetry. This supports the result of RHF/6-31G* calculations.[17] MP2/6-31+G* calculations gave almost the same results as given in ref 23. Optimized structure parameters are listed in Table 1.

At first, the energies of several pseudoconformers were calculated at the RHF/6-31G** level of theory to obtain an approximate potential surface. In the calculations, ϕ_1 and ϕ_2 were fixed at arbitrarily selected values while the other structural parameters were optimized. No minimum was found except for the one at $\phi_1 = \phi_2 = 0°$. It was found that the potential energy, $V(\phi_1,\phi_2)$, is approximately equal to $V(\phi_1,0°) + V(0°,\phi_2)$, showing that the torsions of two phenyl rings are mutually independent.

To obtain as reliable constraints as possible, geometry optimizations of the pseudoconformers were carried out by using MP2/6-31+G* method. In the calculations, the ϕ_2 was fixed at the values taken at intervals of 15° while ϕ_1 was fixed at 0° and the other structural parameters were optimized. This "one-dimensional expansion" of the pseudoconformers was adopted to limit the total computational time to a practical extent referring to the results of the RHF/6-31G** calculations showing the approximate independence of the two phenyl torsions. The constraints of the pseudoconformers of (ϕ_1,ϕ_2) were then derived from those of the pseudoconformers of $(\phi_1,0)$ and $(0,\phi_2)$. The results of the RHF/6-31G** and MP2/6-31+G*calculations are deposited in Tables S2 and S3 and in Tables S4 and S5 in the Supporting Information, respectively.

Cartesian force constants were calculated by BP86 because this method is useful for reproducing the observed vibrational frequencies of *t*-AB.[17] The optimization by BP86/6-31G** calculations assuming molecular symmetry of C_i resulted in a planar structure with C_{2h} symmetry. The result of the optimization is shown in Table 1. Optimized structural parameters and vibrational frequencies are almost the same as those of BP86/6-31G* calculations.[17] The force constants in Cartesian coordinates were converted to the force constants in internal coordinates and were slightly modified by using scale factors.[29] Scale factors for C−H stretching force constants were deter-

TABLE 1: Molecular Structure of *trans*-Azobenzene Determined by Gas Electron Diffraction and the Theoretical Calculations[a]

	experimental[b]				theoretical		
	GED[c]	GED[d]	GED(C_2)[e]	GED(C_i)[f]	RHF/6-31G**	MP2/6-31+G*	BP86/6-31G**[g]
r(N=N)	1.260(8)	1.260(8)	1.261(12)	1.270(12)	1.220	1.279	1.279
r(N−C)	1.427(8)	1.425(8)	1.423(12)	1.430(12)	1.421	1.423	1.421
r(C−C)$_{av}$	1.399(1)	1.399(1)	1.398(3)	1.398(3)	1.386	1.400	1.406
r(C_3−C_4)	1.405	1.405			1.392	1.405	1.415
r(C_4−C_5)	1.393	1.393			1.380	1.395	1.397
r(C_5−C_6)	1.402	1.403			1.390	1.403	1.410
r(C_6−C_7)	1.397	1.396			1.383	1.399	1.404
r(C_7−C_8)	1.396	1.399			1.386	1.397	1.401
r(C_8−C_3)	1.401	1.398			1.385	1.402	1.411
r(C−H)	1.102(7)	1.103(8)	1.087(9)	1.093(9)	1.075	1.088	1.094
∠NNC	113.6(8)	114.2(8)	116.0(12)	114.5(12)	115.7	113.4	114.2
∠NC$_4$	124.7(9)	124.5(9)	121.2(15)	123.0(15)	124.4	124.0	124.9
∠$C_4C_3C_8$	120.5[h]	120.1[i]			120.1	120.7	119.9
∠$C_3C_4C_5$	119.1[h]	119.5[i]			119.5	119.1	119.6
∠$C_3C_8C_7$	119.9[h]	120.2[i]			120.2	119.7	120.2
∠$C_4C_5C_6$	120.6[j]	120.4[j]			120.5	120.5	120.4
∠$C_5C_6C_7$	120.0[j]	120.2[j]			120.0	120.0	120.1
∠$C_6C_7C_8$	119.9[j]	119.7[j]			119.8	119.9	119.8
ϕ_1	0	0	30(5)	28(9)	0	19.5	0

[a] See Figure 1 for atom numbering. [b] r_g in angstroms and $\angle_\alpha$ in degrees. Parenthesized numbers are the estimated limits of error (3σ) in the last significant digits. [c] Present work using the MP2/6-31+G* constraints. Our final conclusion. The index of resolution is 0.94(1). [d] Present work using the RHF/6-31G** constraints. The index of resolution is 0.94(1). [e] C_2 model in ref 9. [f] C_i model in ref 9. [g] C_i symmetry was assumed. [h] Fixed at the MP2/6-31+G* values. [i] Fixed at the RHF/6-31G** values. [j] Dependent parameter.

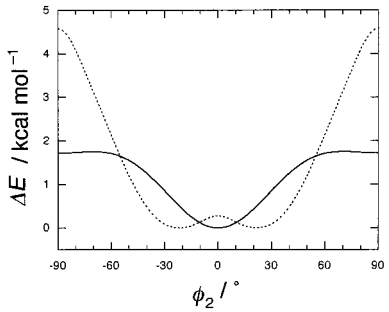

Figure 2. Experimental (solid curve) and theoretical (dashed curve) potential-energy functions for the torsion about N_1−C_9 bond of *trans*-azobenzene relative to the minimum value. The value of ϕ_1 is fixed at 0°. The theoretical function was given by MP2/6-31+G* calculations.

mined to be 0.964 so as to reproduce the vibrational frequencies measured in solutions,[14,15] while it was not necessary to modify the other force constants. Symmetry coordinates, scaled force constants, and the observed and calculated wavenumbers with potential-energy distributions are listed in Tables S6−8 in the Supporting Information.

Analysis of Electron Diffraction Data

The following assumptions were made in the data analysis: (1) the $C_9N_1N_2C_3$ moiety is planar; (2) two phenyl rings are equivalent; (3) the differences between C−C bond lengths are equal to those given by MP2/6-31+G* calculations; (4) the bond angles of phenyl rings, ∠$C_4C_3C_8$, ∠$C_3C_4C_5$, ∠$C_3C_8C_7$, ∠$C_{10}C_9C_{14}$, ∠$C_9C_{10}C_{11}$, and ∠$C_9C_{14}C_{13}$, are equal to those given by MP2/6-31+G* calculations; (5) hydrogen atoms lie on the bisector of the CCC angles; and (6) C−H bond lengths are the same. Under these assumptions, the following structural parameters were used to define the molecular geometry: r(N=N), r(N−C), <r(C−C)>, <r(C−H)>, ∠NNC, and ∠NC_3C_4, where < > denotes an average value.

As shown in Figure 2, the theoretical barrier to the planarity of a phenyl ring is relatively small. Therefore, the torsion of each phenyl ring was treated as a large amplitude vibration by using pseudoconformers. The values of ϕ_1 and ϕ_2 of each pseudoconformer were taken between −90 and 90° at intervals of 15°. As stated in the section of Theoretical Calculations, the torsion of each phenyl ring is approximately independent of each other. On this basis and the consideration of symmetry, the following potential function was adopted for torsion:

$$V(\phi_1,\phi_2) = \Sigma_{i=1,2}\{V_2(1 - \cos 2\phi_i)/2 + V_4(1 - \cos 4\phi_i)/2\} \quad (1)$$

This function can take the minimum at planar ($\phi_1 = \phi_2 = 0$) or nonplanar conformation depending on the values of V_2 and V_4.

In the one-dimensional torsion, the probability distribution, $N \exp(-V(\phi)/RT)$, that is based on the classical approximation is usually used in the analysis of GED data, where N is a normalization factor. If this formulation can be applied to the two-dimensional case, the relative abundance, $P(\phi_1, \phi_2)$, of each pseudoconformer is calculated as

$$P(\phi_1, \phi_2) = N \exp(-V(\phi_1, \phi_2)/RT) \quad (2)$$

From the molecular symmetry, ϕ_1 and ϕ_2 couple to make linear combinations, $\alpha = (\phi_1 + \phi_2)/\sqrt{2}$ and $\beta = (\phi_1 - \phi_2)/\sqrt{2}$, that belong to A_u and B_g species of the point group C_{2h}, respectively (they correspond to S_{47} and S_{48} in Tables S6 and S7, respectively). The reduced mass for α is quite different from that for β because the coordinate β couples with the overall rotation of the molecular frame[30] and consequently, the vibrational frequency of β is about four times as high as that of α (see Table S8).

This effect is not included in eq 2 explicitly, but it is difficult to derive the exact formula of $P(\phi_1, \phi_2)$ in classical mechanics. Therefore, quantum mechanical calculations were carried out to obtain the wave function $\phi_n(\phi_1, \phi_2)$ and the energy E_n by using the potential function of eq 1. Then the probability distribution was calculated as

$$P(\phi_1, \phi_2) = N \Sigma_n \phi_n(\phi_1,\phi_2)^* \phi_n(\phi_1,\phi_2) \exp(-E_n/RT) \quad (3)$$

and the result was compared with that of eq 2 to examine the

validity of the latter. The Hamiltonian used is

$$H = -\left(\frac{\partial}{\partial\phi_1}\frac{\partial}{\partial\phi_2}\right)\begin{pmatrix}B_{11} & B_{12}\\ B_{12} & B_{11}\end{pmatrix}\begin{pmatrix}\frac{\partial}{\partial\phi_1}\\ \frac{\partial}{\partial\phi_2}\end{pmatrix} + V(\phi_1,\phi_2) \qquad (4)$$

where the kinetic-energy term was approximated by the following expansion:

$$B_{11} = B_{11}^{(0)} + B_{11}^{(20)}\cos(2\phi_1) + B_{11}^{(20)}\cos(2\phi_2) + B_{11}^{(22)}\cos(2\phi_1)\cdot\cos(2\phi_2)$$

$$B_{12} = B_{12}^{(0)} + B_{12}^{(20)}\cos(2\phi_1) + B_{12}^{(20)}\cos(2\phi_2) + B_{12}^{(22)}\cos(2\phi_1)\cdot\cos(2\phi_2) \quad (5)$$

The expansion coefficients, $B_{11}^{(0)}$, $B_{11}^{(20)}$, and so forth are functions of moment of inertia of the molecule and internal rotors, and they were evaluated by using a method similar to that described in ref 31. The products of free rotation eigenfunctions, $\exp(in\phi_1)\cdot\exp(im\phi_2)/2\pi$, for $n, m = -15$ to 15 were used as a basis set. The quantum mechanical calculations (eq 3) provided essentially the same distribution as eq 2. However, the very long computation time of the quantum mechanical calculations makes it unrealistic to use them in least-squares iteration to determine potential constants. Therefore, we concluded to adopt eq 2 with no correction in the present study.

Mean amplitudes and shrinkage corrections of each pseudoconformer were calculated by using the scaled force constants of the planar form. Calculated mean amplitudes are listed in Table 2. Asymmetry parameters, κ, were estimated by the conventional method.[32] Mean amplitudes were refined in groups divided according to the positions of peaks in a radial distribution function as (i) $r_a < 1.7$ Å, (ii) $r_a = 1.7-2.6$ Å, (iii) $r_a = 2.6-3.1$ Å, (iv) $r_a = 3.1-5.2$ Å, and (v) $r_a > 5.2$ Å.

According to MP2/6-31+G* calculations, the changes in the following bond lengths and bond angles are greater than 0.003 Å and 0.3°, respectively, during the rotation about N_1-C_9 bond: the C=C distances and the CCC angles in the phenyl ring bonded to N_1 atom, $r(N_1=N_2)$, $r(N_1-C_9)$, $r(N_2-C_3)$, $\angle N_2N_1C_9$, $\angle N_1C_9C_{10}$, and $\angle N_1C_9C_{14}$. The structural differences between pseudoconformers were fixed at the values obtained from MP2/6-31+G* calculations except for $\angle N_1C_9C_{10}$ and $\angle N_1C_9C_{14}$. The tilt angle of the phenyl ring, which is defined as $\tau = (\angle N_1C_9C_{10} - \angle N_1C_9C_{14})/2$, equals 0° when the phenyl ring rotates by 90°. The ratios of this parameter between pseudoconformers, $[\tau(\phi)/\tau(0°)]$, were fixed at the theoretical values. The changes in the above structural parameters caused by the torsions of the phenyl rings were assumed to be additive for the torsions of two rings except for $\angle N_1C_9C_{10}$ and $\angle N_1C_9C_{14}$. Structural parameters, mean amplitudes, the index of resolution, and potential constants were determined by least-squares calculations on molecular scattering intensities.

TABLE 2: Interatomic Distances, Calculated and Observed Mean Amplitudes for the Pseudoconformer with $\phi_1 = \phi_2 = 0°$ of *trans*-Azobenzene[a]

atom pair	r_a	l_{calc}[b]	l_{obs}	group[c]
<C−H>	1.097	0.077	0.078(1)	1
$N_1=N_2$	1.259	0.041	0.042	1
C_4-C_5	1.391	0.045	0.046	1
C_6-C_7	1.395	0.046	0.047	1
C_3-C_8	1.399	0.046	0.047	1
C_7-C_8	1.394	0.046	0.047	1
C_5-C_6	1.400	0.046	0.047	1
C_3-C_4	1.403	0.047	0.048	1
N_2-C_3	1.425	0.050	0.051	1
$N_1\cdots C_3$	2.243	0.059	0.063(2)	2
$N_1\cdots C_{14}$	2.377	0.065	0.070	2
$C_3\cdots C_5$	2.406	0.057	0.062	2
$C_6\cdots C_8$	2.412	0.057	0.062	2
$C_5\cdots C_7$	2.416	0.057	0.062	2
$C_3\cdots C_7$	2.415	0.057	0.062	2
$C_4\cdots C_8$	2.427	0.057	0.062	2
$C_4\cdots C_6$	2.422	0.057	0.062	2
$N_1\cdots C_{10}$	2.503	0.064	0.069	2
$N_1\cdots C_4$	2.722	0.098	0.102(4)	3
$C_5\cdots C_8$	2.783	0.065	0.070	3
$C_3\cdots C_6$	2.785	0.064	0.069	3
$C_4\cdots C_7$	2.800	0.065	0.070	3
$N_1\cdots C_8$	3.486	0.063	0.075(7)	4
$C_3\cdots C_9$	3.536	0.064	0.077	4
$N_2\cdots C_7$	3.668	0.066	0.079	4
$N_2\cdots C_5$	3.742	0.066	0.079	4
$N_1\cdots C_5$	4.104	0.101	0.114	4
$C_3\cdots C_{10}$	4.139	0.105	0.118	4
$N_1\cdots C_{12}$	4.200	0.070	0.082	4
$C_3\cdots C_{14}$	4.611	0.079	0.092	4
$N_1\cdots C_7$	4.650	0.070	0.083	4
$C_4\cdots C_{14}$	4.887	0.145	0.158	4
$N_1\cdots C_6$	4.898	0.088	0.101	4
$C_4\cdots C_{10}$	5.066	0.104	0.116	4
$C_3\cdots C_{11}$	5.516	0.108	0.139(20)	5
$C_8\cdots C_{14}$	5.822	0.079	0.110	5
$C_3\cdots C_{13}$	5.884	0.075	0.106	5
$C_5\cdots C_{14}$	6.252	0.162	0.194	5
$C_4\cdots C_{13}$	6.256	0.139	0.170	5
$C_3\cdots C_{12}$	6.263	0.087	0.119	5
$C_4\cdots C_{11}$	6.389	0.104	0.136	5
$C_4\cdots C_{12}$	6.901	0.116	0.147	5
$C_8\cdots C_{13}$	7.011	0.087	0.119	5
$C_8\cdots C_{12}$	7.196	0.127	0.159	5
$C_5\cdots C_{13}$	7.622	0.154	0.186	5
$C_5\cdots C_{11}$	7.728	0.104	0.136	5
$C_7\cdots C_{13}$	8.257	0.082	0.114	5
$C_5\cdots C_{12}$	8.274	0.118	0.150	5
$C_7\cdots C_{12}$	8.526	0.113	0.145	5
$C_6\cdots C_{12}$	9.004	0.097	0.128	5

[a] Distances and amplitudes in angstroms. See Figure 1 for atom numbering. Nonbonded atom pairs including hydrogen atom are not listed. Parenthesized numbers are estimated limits of error (3σ) in the last significant digits. [b] Calculated at 407 K. [c] The mean amplitudes with the same number were refined as one group. The differences between the mean amplitudes in each group were fixed at calculated values.

Results and Discussion

Molecular scattering intensities and a radial distribution curve are shown in Figures 3 and 4, respectively. Experimental structural parameters and mean amplitudes are listed in Tables 1 and 2, respectively. Potential constants, V_2 and V_4, in eq 1 were determined to be 1.7(6) and 0.6(13) kcal mol^{-1}, respectively, where parenthesized numbers denote three times the standard deviations. The determined potential function is displayed in Figure 2, showing that the conformation of *t*-AB is planar. Care must be paid for the uncertainties of V_2 and V_4. If V_4 is larger than $-V_2/4$, the potential function $V(0°, \phi_2)$ has a minimum at the point of $\phi_2 = 0°$. Figure 5 shows this region along with the ellipses corresponding to 2σ and 3σ. They are drawn by using the standard deviations and the correlation coefficient of V_2 and V_4. A numerical integration shows that *t*-AB takes a planar conformation at the 99.1% confidence interval. The absolute values of correlation matrix elements are less than 0.7 except for $r(N-C)/r(C-C) = -0.79$. The correlation matrix is given in Table S9 as the Supporting Information.

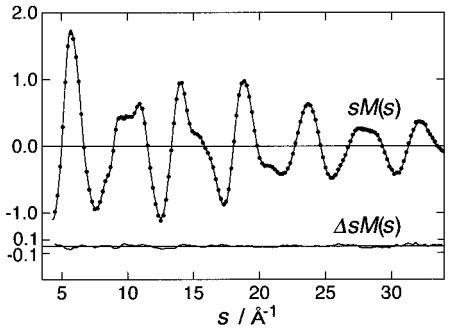

Figure 3. Experimental (dots) and theoretical (solid curve) molecular scattering intensities of *trans*-azobenzene; $\Delta sM(s) = sM(s)^{obs} - sM(s)^{calc}$. The theoretical curve was calculated from the best fitting parameters.

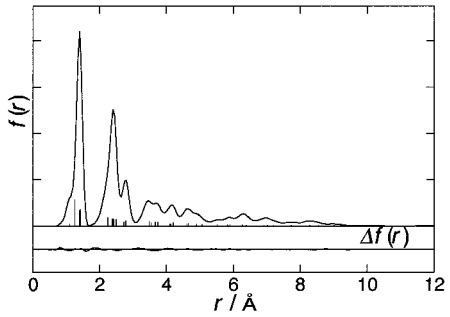

Figure 4. Experimental radial distribution curve of *trans*-azobenzene; $\Delta f(r) = f(r)^{obs} - f(r)^{calc}$. Vertical bars indicate relatively important atom pairs of the molecule when ϕ_1 and ϕ_2 equal 0°.

The data analysis was also performed using the structural constraints given by RHF/6-31G** calculations. The results agree within experimental uncertainties with those given by the analysis with MP2/6-31+G* constraints, although the errors of the former are slightly larger than those of the latter.

Structural Parameters of *t*-AB. As shown in Table 1, the uncertainties of the structural parameters are smaller than those in the previous GED study.[9] Most of the structural parameters determined in the present study agree with the previous ones. However, the bond angles significantly differ from the previous ones determined by assuming C_2 symmetry.

The solid-phase values of r(N═N), r(N−C), $<r$(C−C)$>$, ∠NNC, and ∠NCC$_4$ determined at 82 K[13] are 1.259(1.251), 1.431(1.431), 1.395(1.395) Å, 113.5(114.1), and 123.5(124.4)°, respectively. The values in parentheses show the parameter values of the molecule at the site where disorder was found at room temperature.[13] The values in both sites are similar to the corresponding gas-phase values, 1.260(8), 1.427(8), 1.399(1) Å, 113.6(8), and 124.7(9)°.

A comparison of the theoretical structure parameters with the observed ones reveals the following points (see Table 1). (1) The RHF/6-31G** calculation gives too short N═N and C−C distances. The MP2/6-31+G* and BP86/6-31G** calculations overestimate these distances, but the deviations are small as compared with the RHF/6-31G** calculation. (2) Each of the theoretical N−C distances agrees with the experimental distance. (3) The RHF/6-31G** calculation overestimates ∠NNC but reproduces ∠N$_2$C$_3$C$_4$ well. (4) The bond angles given by the MP2/6-31+G* and BP86/6-31G** calculations agree with the observed ones.

Conformation and Torsional Barrier of *t*-AB. The planar conformation determined in the present study differs from the stable conformation in the previous GED study.[9] This is perhaps ascribable to the difference in the treatment of phenyl torsions.

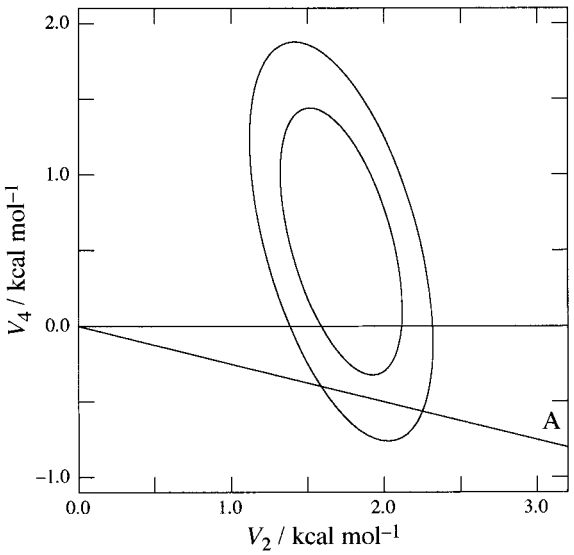

Figure 5. Experimental values with uncertainties of potential-energy constants. Only the values of V_2 and V_4 above line A correspond to the planar form. Two ellipses correspond to 2σ and 3σ, respectively.

The dihedral angle of 30° given by the previous study is a consequence of the treatment in which the torsions of phenyl rings were approximated as small amplitude vibrations and is not real. As stated in ref 9, the stable conformation of *t*-AB is considered to be mainly determined by the following factors: the conjugation between the azo and phenyl groups making the molecule planar and the repulsion between the hydrogen atom and the lone-pair electrons in the nitrogen atom distorting the molecular plane. The fact that the structure of *t*-AB is planar shows that the former is dominant. The experimental N$_1$···H$_{15}$ distance in the planar structure is determined to be 2.47 Å, which is not much smaller than the sum of the van der Waals radii of nitrogen and aromatic hydrogen atoms (1.55 and 1.0 Å[33]). Thus, the steric repulsion between these atoms does not seem so strong. In the crystal phase at 82 K, *t*-AB is not planar with the dihedral angle of 10 or 20°,[13] suggesting the packing effect in the crystal.

As shown in Figure 2, the experimental potential function disagrees with the theoretical one. The torsional barrier of a phenyl ring obtained by RHF/6-31G** calculations, 5.2 kcal mol^{-1}, is nearly three times as large as the experimental one, 1.7(6) kcal mol^{-1}. This overestimation is similar to the case of *t*-AXB[4] and nitrobenzene.[34−36] In the MP2/6-31+G* calculations, the potential barrier where one of the phenyl groups is perpendicular to the molecular plane is 4.7 kcal mol^{-1} and the barrier of the double minimum potential is 0.4 kcal mol^{-1}. Whether this molecule has a double minimum with a low barrier is left for future investigations.

Comparison of the Molecular Structure of *t*-AB with That of *t*-AXB. The structures of *t*-AB and *t*-AXB are compared in Table 3. The structure of *t*-AXB is also planar.[4] The N$_1$N$_2$C$_3$ angle, 121.3(12)°, and the tilt angle of the phenyl ring attached to the N$_2$ atom, 9.0(14)°, of *t*-AXB[4] are larger than the corresponding angles of *t*-AB by 7.7(15) and 4.0(16)°, respectively. The differences can be ascribed to the steric repulsion between the O and H$_{15}$ atoms in *t*-AXB. The N−C bond length of *t*-AB, 1.427(8) Å, is shorter than the average length of the two N−C bonds in *t*-AXB, 1.438(7) Å.[4] The difference of about 0.01 Å is consistent with the results of RHF/6-31G** calculations, in which the N−C length of *t*-AB is 1.421 Å and the average N−C length of *t*-AXB is 1.432 Å.[4]

TABLE 3: Comparison of the Molecular Structure of *trans*-Azobenzene (*t*-AB) and *trans*-Azoxybenzene (*t*-Axb)[a]

	t-AB	*t*-AXB[b]	
$r_g(N_1{=}N_2)$	1.260(8)	1.271	(3)
$r_g(O{-}N_1)$		1.271	
$r_g(N_1{-}C_9)$	1.427(8)	1.464	(7)
$r_g(N_2{-}C_3)$		1.414	
$<r_g(C{-}C)>$[c]	1.399(1)	1.400(1)	
$<r_g(C{-}H)>$[c]	1.102(7)	1.100(6)	
$\angle_\alpha N_1N_2C_3$	113.6(8)	121.3(13)	
$\angle_\alpha N_2N_1C_9$		113.3(19)	
$\tau(C_3)$[d]	5.0(9)	9.0(14)	
$\tau(C_9)$[e]		2.6(23)	

[a] See Figure 1 for atom numbering. r_g in angstroms and angles in degrees. Numbers in parentheses are the estimated limits of error (3σ). [b] Reference 4. [c] Average value. [d] Tilt angle of the phenyl ring bonded to the C_3 atom, which is defined as $\tau(C_3) = (\angle_\alpha N_2C_3C_4 - \angle_\alpha N_2C_3C_8)/2$. [e] Tilt angle of the phenyl ring bonded to the C_9 atom, which is defined as $\tau(C_9) = (\angle_\alpha N_1C_9C_{10} - \angle_\alpha N_1C_9C_{14})/2$.

The potential barriers for torsion around the $N_2{-}C_3$ and $N_1{-}C_9$ bonds of *t*-AXB are determined to be 1.7(10) and 3.5(16) kcal mol^{-1}, respectively.[4] The former agrees with that of *t*-AB, 1.7(6) kcal mol^{-1}, within the limits of error, but the latter is about twice as large as it.

T_{N-I} of Liquid Crystals with the Core of *t*-AB Type. The liquid crystal is considered to have the stable nematic phase if T_{N-I} is high. As stated in the Introduction, if the terminal groups are the same, the T_{N-I} of the liquid crystal with the *t*-AB type core is generally lower than those of the liquid crystals with *t*-AXB and *trans*-stilbene (*t*-SB) type cores by about 20 °C and 30 °C, respectively.[6,7] The structure of *t*-SB has been found to be planar, and the barrier for torsion of each phenyl ring of *t*-SB has been determined to be 2.5 kcal mol^{-1} by dispersed fluorescence spectroscopy.[37] Therefore, each of *t*-AB, *t*-AXB, and *t*-SB has a planar structure. Moreover, the barrier of *t*-SB is not much different from that of *t*-AB, 1.7(6) kcal mol^{-1}, and the barriers of *t*-AXB, 1.7(10) and 3.5(16) kcal mol^{-1}. Thus, the origin of the differences in the T_{N-I} of liquid crystals with these types of cores is neither the planarity of the core nor the torsional barriers of the phenyl rings in the core.

A possible origin is the different length of the linking unit (r_{lu}) connecting two phenyl groups because it is known that the liquid crystalline phase is stabilized as r_{lu} increases.[38] The determined r_{lu} ($C_3{\cdots}C_9$ distance) of *t*-AB, 3.54 Å, is smaller than the r_{lu} of *t*-SB, 3.92 Å, determined by GED.[39] Therefore the difference in the r_{lu} is considered to be the origin of the difference, 30 °C, in the T_{N-I} between the liquid crystals with the cores of *t*-AB and *t*-SB types. On the other hand, the r_{lu} of *t*-AXB has been determined to be 3.62 Å. The difference of 0.1 Å seems to explain only a part of 20 °C, the difference between the T_{N-I} of the liquid crystals with the cores of *t*-AB and *t*-AXB types.

Another explanation in terms of polarity is possible. The *t*-AB molecule is nonpolar, and the *t*-AXB molecule is polar. The oxygen atom of *t*-AXB has a fairly large negative charge, about $-0.6\,e$, according to RHF/6-31G** calculations. Such a charged atom gives intermolecular dipolar interactions and would stabilize the liquid crystalline phase.[40] Therefore, the dipolar interactions in addition to the increase in r_{lu} are considered to raise the T_{N-I} of the liquid crystal with the core of *t*-AXB type.

Acknowledgment. We thank the Computer Center, Institute for Molecular Science, Okazaki National Research Institutes, for the use of the NEC HPC computer and the GAUSSIAN 94 and 98 programs. Data analysis was performed using the HITAC MP5800/160 at the Hokkaido University Computing Center. RHF/6-31G** calculations were performed using the SUN Ultra Enterprise 4000 computer and the GAUSSIAN 94 program at the Hokkaido University Computing Center.

Supporting Information Available: Tables of the leveled total intensities and the backgrounds (Table S1), the optimized geometrical parameters of the stable and pseudoconformers (Tables S2−5), the local symmetry coordinates (Table S6), the force constants (Table S7), the observed and calculated frequencies with potential-energy distributions (Table S8), and the correlation matrix (Table S9). Supporting Information is available free of charge via the Internet at http://pubs.acs.org.

References and Notes

(1) Kuze, N.; Ebizuka, M.; Fujiwara, H.; Takeuchi, H.; Egawa, T.; Konaka, S.; Fogarasi, G. *J. Phys. Chem. A* **1998**, *102*, 2080.
(2) Kuze, N.; Fujiwara, H.; Takeuchi, H.; Egawa, T.; Konaka, S.; Fogarasi, G. *J. Phys. Chem. A* **1999**, *103*, 3054.
(3) Gray, G. W. In *The Molecular Physics of Liquid Crystals*; Luckhurst, G. R., Gray, G. W., Eds.; Academic Press: London, 1979; Chapter 1.
(4) Tsuji, T.; Takashima, H.; Takeuchi, H.; Egawa, T.; Konaka, S. *J. Mol. Struct.* **2000**, *554*, 203.
(5) Traetteberg, M.; Hilmo, I.; Abraham, R. J.; Ljunggren, S. *J. Mol. Struct.* **1978**, *48*, 395.
(6) Knaak, L. E.; Rosenberg, H. M.; Servé, M. P. *Mol. Cryst. Liq. Cryst.* **1972**, *17*, 171.
(7) Thiemann, T.; Vill, V. *Liq. Cryst.* **1997**, *22*, 519.
(8) Vill, V. In *Landolt-Börnstein*; Thiem, J., Ed.; New Series; Springer-Verlag: Berlin, 1992; Vol. IV/7.
(9) Traetteberg, M.; Hilmo, I.; Hagen, K. *J. Mol. Struct.* **1977**, *39*, 231.
(10) De Lange, J. J.; Robertson, J. M.; Woodward, I. *Proc. R. Soc. London, Ser. A* **1939**, *171*, 398.
(11) Brown, C. J. *Acta Crystallogr.* **1966**, *21*, 146.
(12) Bouwstra, A.; Schouten, A.; Kroon, J. *Acta Crystallogr.* **1983**, *C39*, 1121.
(13) Harada, J.; Ogawa, K.; Tomoda, S. *Acta Crystallogr.* **1997**, *B53*, 662.
(14) Kellerer, B.; Hacker, H. H.; Brandmüller, J. *Indian J. Pure Appl. Phys.* **1971**, *9*, 903.
(15) Gruger, A.; Le Calvé, N.; Dizabo, P. *J. Chim. Phys.* **1972**, *69*, 291.
(16) Armstrong, D. R.; Clarkson, J.; Smith, W. E. *J. Phys. Chem.* **1995**, *99*, 17825.
(17) Biswas, N.; Umapathy, S. *J. Phys. Chem. A* **1997**, *101*, 5555.
(18) Scott, A. P.; Radom, L. *J. Phys. Chem.* **1996**, *100*, 16502.
(19) Mohandas, P.; Umapathy, S. *J. Phys. Chem. A* **1997**, *101*, 4449.
(20) Magdó, I.; Németh, K.; Mark, F.; Hildebrandt, P.; Schaffner, K. *J. Phys. Chem. A* **1999**, *103*, 289.
(21) Becke, A. D. *Phys. Rev. A* **1988**, *38*, 3098.
(22) Perdew, J. P. *Phys. Rev. B* **1986**, *33*, 8822.
(23) Kurita, N.; Tanaka, S. *J. Phys. Chem. A* **2000**, *104*, 8114.
(24) Konaka, S.; Kimura, M. In *13th Austin Symposium on Gas-Phase Molecular Structure*, The University of Texas, Austin, TX, March 12−14, 1990; S21.
(25) Tsuboyama, A.; Murayama, A.; Konaka, S.; Kimura, M. *J. Mol. Struct.* **1984**, *118*, 351.
(26) Kimura, M.; Konaka, S.; Ogasawara, M. *J. Chem. Phys.* **1967**, *46*, 2599.
(27) Tavard, C.; Nicolas, D.; Rouault, M. *J. Chim. Phys. Phys.-Chim. Biol.* **1967**, *64*, 540.
(28) (a) Frisch, M. J.; Trucks, G. W.; Schlegel, H. B.; Gill, P. M. W.; Johnson, B. G.; Robb, M. A.; Cheeseman, J. R.; Keith, T.; Petersson, G. A.; Montgomery, J. A.; Raghavachari, K.; Al-Laham, M. A.; Zakrzewski, V. G.; Ortiz, J. V.; Foresman, J. B.; Cioslowski, J.; Stefanov, B. B.; Nanayakkara, A.; Challacombe, M.; Peng, C. Y.; Ayala, P. Y.; Chen, W.; Wong, M. W.; Andres, J. L.; Replogle, E. S.; Gomperts, R.; Martin, R. L.; Fox, D. J.; Binkley, J. S.; Defrees, D. J.; Baker, J.; Stewart, J. P.; Head-Gordon, M.; Gonzalez, C.; Pople, J. A. *GAUSSIAN 94*; Gaussian, Inc.: Pittsburgh, PA, 1995. (b) Frisch, M. J.; Trucks, G. W.; Schlegel, H. B.; Scuseria, G. E.; Robb, M. A.; Cheeseman, J. R.; Zakrzewski, V. G.; Montgomery, J. A., Jr.; Stratmann, R. E.; Burant, J. C.; Dapprich, S.; Millam, J. M.; Daniels, A. D.; Kudin, K. N.; Strain, M. C.; Farkas, O.; Tomasi, J.; Barone, V.; Cossi, M.; Cammi, R.; Mennucci, B.; Pomelli, C.; Adamo, C.; Clifford, S.; Ochterski, J.; Petersson, G. A.; Ayala, P. Y.; Cui, Q.; Morokuma, K.; Malick, D. K.; Rabuck, A. D.; Raghavachari, K.; Foresman, J. B.; Cioslowski, J.; Ortiz, J. V.; Baboul, A. G.; Stefanov, B. B.; Liu, G.; Liashenko, A.; Piskorz, P.; Komaromi, I.; Gomperts, R.; Martin, R. L.; Fox, D. J.; Keith, T.; Al-Laham, M. A.; Peng, C. Y.; Nanayakkara, A.;

Challacombe, M.; Gill, P. M. W.; Johnson, B.; Chen, W.; Wong, M. W.; Andres, J. L.; Gonzalez, C.; Head-Gordon, M.; Replogle, E. S.; Pople, J. A. *GAUSSIAN 98*, Revision A.9; Gaussian, Inc.: Pittsburgh, PA, 1998.

(29) Pulay, P.; Fogarasi, G.; Pongor, G.; Boggs, J. E.; Vargha, A. *J. Am. Chem. Soc.* **1983**, *105*, 7037.

(30) Hadder, J. E.; Frederick, J. H. *J. Chem. Phys.* **1992**, *97*, 3500.

(31) Harthcock, M. A.; Laane, J. *J. Mol. Spectrosc.* **1982**, *91*, 300.

(32) Kuchitsu, K.; Bartell, L. S. *J. Chem. Phys.* **1961**, *35*, 1945.

(33) Bondi, A. *J. Phys. Chem.* **1964**, *68*, 441.

(34) Høg, J. H.; Nygaard, L.; Sørensen, G. O. *J. Mol. Struct.* **1970**, *7*, 111.

(35) Carreira, L. A.; Towns, T. G. *J. Mol. Struct.* **1977**, *41*, 1.

(36) Domenicano, A.; Schultz, G.; Hargittai, I.; Colapietro, M.; Portalone, G.; George, P.; Bock, C. W. *Struct. Chem.* **1990**, *1*, 107.

(37) Chiang, W.-Y.; Laane, J. *J. Chem. Phys.* **1994**, *100*, 8755.

(38) Verbit, L.; Tuggey, R. L. In *Liquid Crystals and Ordered Fluids*, Johnson J. F., Porter, R. S., Eds.; Plenum Press: New York, 1973; Vol. 2, 309.

(39) Traetteberg, M.; Frantsen, E. B.; Mijlhoff, F. C.; Hoekstra, A. *J. Mol. Struct.* **1975**, *26*, 57.

(40) van der Veen, J.; de Jeu, W. H.; Grobben, A. H.; Boven, J. *Mol. Cryst. Liq. Cryst.* **1972**, *17*, 291.